C.P. No. 972

MINISTRY OF TECHNOLOGY

AERONAUTICAL RESEARCH COUNCIL

CURRENT PAPERS

Guided Weapons Aerodynamic Study

Force and Moment Measurements on some Monoplane and Cruciform Slender Wing-Body Combinations at M = 4.0

by

P. L. Roe

LONDON: HER MAJESTY'S STATIONERY OFFICE

1968

PRICE 5*s* 6*d* NET

U.D.C. No. 533.665 : 533.695.12 : 533.693.3 : 533.6.013.13/15 :
533.693.9 : 533.652.1 : 533.6.011.5

C.P. No.972*
October 1966

GUIDED WEAPONS AERODYNAMIC STUDY

FORCE AND MOMENT MEASUREMENTS ON SOME MONOPLANE AND CRUCIFORM SLENDER WING-BODY COMBINATIONS AT M = 4.0

by

P. L. Roe

SUMMARY

Force and moment measurements are presented for a family of slender delta monoplane wings (aspect ratios 0.826, 0.517, 0.309, 0.229) in combination with a common ogive-cylinder body. Two of these (aspect ratios 0.826 and 0.309) are also studied in cruciform layout. Results are given for variations in incidence at zero roll, and variations in roll at constant pitch. Longitudinal characteristics are compared with an empirical prediction method, and with test results at lower Mach numbers.

---

*Replaces R.A.E. Technical Report No.66342 - A.R.C. 28708.

CONTENTS

1 INTRODUCTION

This Paper is an addition to the systematic study of simple missile configurations being undertaken at R.A.E. Bedford. The particular contribution made here is the study at M = 4 of a family of configurations consisting of different slender delta wings in combination with a standard ogive-cylinder body. Four monoplane and two cruciform layouts are considered.

2 EQUIPMENT AND TEST PROCEDURES

2.1 Model details

Drawings of the models tested are shown in Fig.1. They were constructed from a set of standard parts, and all in this series made use of the same body, known in the Bedford programme as B_{1a}. This has a nose section, three body diameters in length, having very nearly* the shape of a tangent ogive, followed by a parallel section ten diameters long.

To this body could be added one of three sets of delta wings, known as wings 7, 8 and 9. Each wing has the same root chord, equal to 9.6825 diameters. The wings all have leading edges which are, at M = 4, swept well within the Mach cone, as is shown by calculating values of the parameter $\sqrt{M^2-1}\cot\phi$, where ϕ is the leading edge sweep angle.

Wing	$\sqrt{M^2-1}\cot\phi$
7	0.5
8	0.3
9	0.2234

This Paper also includes data, taken from Ref.1, on the body alone, and on a fourth configuration, using the same body with a wing of the same root chord but wider span, for which $\sqrt{M^2-1}\cot\phi = 0.8$ (wing 1).

Two cruciform configurations were tested, one having two pairs of wings 1, and the other two pairs of wings 8.

For convenience, the combination of wings 7 with the standard body, for example, will be referred to as model $B_{1a}W_7$, and the combination of two pairs of wings 1 with the standard body as model $XB_{1a}W_1$.

To fix boundary layer transition, roughness was applied in the form of 60-grade carborundum particles embedded in a thin film of Araldite. This treatment was applied over a strip lying between 1/16 inch and 5/16 inch from

---

*The actual shape is given by $(r/d) = -0.002615\,(x/d)^3 - 0.039867\,(x/d)^2 + 0.30984\,(x/d)$, where x is measured from the tip of the nose.

the wing leading edge and over a band between 1/4 inch and 1/2 inch from the tip of the body nose. This treatment had previously been found[1] to give a variation of zero-lift drag with Reynolds number on $B_{1a}W_1$ that was consistent with turbulent flow.

2.2 Scope of tests

All the monoplane configurations were tested over a range of incidence, -5° to $+25^\circ$, except for the highest aspect ratio layout ($B_{1a}W_1$), which could not be set at more than 20° incidence without exceeding the maximum balance load. The cruciform configurations were tested over a similar range, both at zero roll and 45° roll. Each configuration was also tested over a range of roll angles at pitch attitudes $0(5)25^\circ$. The monoplanes were tested over a roll range $0\text{-}90^\circ$, and the cruciform models over a range $0\text{-}45^\circ$, it being assumed that the remainder of the range could in each case be determined from symmetry. Occasional spot checks verified this assumption.

The tests were all carried out with the models sting mounted in the 3 ft x 4 ft tunnel (H.S.S.T.) at R.A.E. Bedford, at a nominal Mach number of 4.0 (actually 3.97). The Reynolds number based on model length was 31.2×10^6, rather higher than that of the corresponding tests at lower Mach number described in Ref.2.

2.3 Corrections to and accuracy of results

All results are corrected for sting deflection, balance interaction, and errors in tunnel flow direction. The observed axial force has been corrected to a standard condition in which base pressure equals free stream static pressure.

The reference area for force coefficients is taken as the cross-sectional area of the parallel portion of the body, and the reference length for moments is the body diameter.

The accuracy of the results has been estimated as within the following limits. (See list of symbols.)

		$\alpha = 0$	$\alpha = 20^\circ$
α		$\pm 0.1^\circ$	
β		$\pm 0.1^\circ$	
M		± 0.02	
C_z		± 0.1	± 0.3
C_x		± 0.02	± 0.02
C_ℓ		± 0.1	± 0.1
$x_{c.p.}/d$	$B_{1a}W_1$	± 0.1	± 0.05
	B_{1a}	± 0.5	

The accuracy with which the position of the centre of pressure near zero incidence can be determined diminishes as the wing size decreases.

3 RESULTS AND DISCUSSION

3.1 Longitudinal characteristics

Normal force ($-C_z$) is plotted against incidence for each of the four monoplane wing-body combinations, and for the body alone, in Fig.3. The data for B_{1a} and $B_{1a}W_1$ are taken from Ref.1.

Also included in this figure are curves derived using an empirical prediction method similar to that described in Ref.2. The essence of this method is to evaluate the normal force acting on the body nose by shock-expansion theory, and the force which would act on the isolated wing by Collingbourne's method[3]. The additional force experienced by the wing due to the presence of the body, and the force carried by the body due to the presence of the wing, are both estimated using the interference factors calculated in Ref.4 for the low incidence case. The present calculations differ from Ref.2 in assuming that when wings are present they prevent the development of any sizeable non-linear force on the body due to body vortex separation. In Ref.2 the opposite assumption is made, that such a non-linear component is always present, of the same magnitude as on the isolated body. It is currently thought that the present method is more appropriate to high Mach numbers, but work is in hand to clarify this point[5].

In calculating the forces on the isolated body, the non-linear component has been allowed for, and calculated on the basis of Allen's[6] cross-flow theory, as amended in Ref.7. It will be observed that agreement is good, the greatest errors being about 8% for the wing-body combinations, and about 12% for the body alone.

Estimates of the initial lift curve slope were made using linear theory for the wings, shock-expansion theory for the body, and Ref.4 for the interference forces. Experimental values of this slope were found by finding, in effect, the best fitting curve of the general form

$$-C_z = a\alpha + b\alpha\,|\alpha|$$

to the experimental points lying between -4° and $+4^\circ$ incidence. This was done by plotting values of the expression

$$\{(-C_z)_{\alpha=\alpha_1} - (-C_z)_{\alpha=-\alpha_1}\}/2\alpha_1$$

against α_1. The resulting graph was always close to a straight line. Fitting a good straight line by eye, and extrapolating it to $\alpha_1 = 0$ gave a value for the coefficient 'a', which could be estimated as accurate to within ±3%. Excellent agreement is achieved between observed and calculated values of the initial lift curve slope, as may be seen from the table below:-

	$-\left(\frac{dC_z}{d\alpha}\right)_{\alpha=0}$	
	Estimate	Experiment
B_{1a}	3.42	3.43
$B_{1a}W_9$	8.0	8.0
$B_{1a}W_8$	10.7	11.2
$B_{1a}W_7$	18.1	18.2
$B_{1a}W_1$	32.4	32.4

The curves of $(-C_z)$ vs α are noticeably more non-linear for the lower aspect ratio configurations. This is demonstrated by calculating the percentage of non-linear lift acting at 20° incidence from the expression

$$\frac{(-C_z)_{\alpha=20^\circ} - \left(-\frac{dC_z}{d\alpha}\right)_{\alpha=0} \times 20 \times \frac{\pi}{180}}{(-C_z)_{\alpha=20^\circ}}$$

which yields the following values:-

	% non-linear lift at $\alpha = 20^\circ$
B_{1a}	62.5
$B_{1a}W_9$	50.9
$B_{1a}W_8$	40.8
$B_{1a}W_7$	30.4
$B_{1a}W_1$	10.3

These values contrast with the results obtained by Andrews[1] for a family of configurations using the same body as in the present tests, but wings of

constant span (= 5d) and varying root chord (9.68d, 7.74d, 6.46d). None of these combinations departed from a linear ($-C_z$, α) relationship by more than about 12%.

In Fig.4 results are presented for the two cruciform configurations. When either of these was set at incidence with one pair of wings in the incidence plane (roll angle = λ = 0), the normal force variation with incidence was indistinguishable from that of the corresponding monoplane. When the model was set so that the incidence plane bisected the right angle between the wings ($\lambda = 45^\circ$), the normal force* changed slightly, being increased by about 6% in the case of $XB_{1a}W_1$, and very slightly decreased in the case of $XB_{1a}W_8$.

In Fig.5(a) the measured centres of pressure of monoplane layouts are compared with estimates made using the methods outlined earlier. Agreement is quite good, and well within the claimed accuracy of the method, except for the case of the body alone. Here the estimate is sometimes in error by as much as two calibres, probably as a result of using a mathematical model which over-simplified the manner in which vortex development takes place. It will be observed that centre of pressure travel increases as wing size diminishes.

In Fig.5(b) the centres of pressure are shown for the two cruciform layouts. At λ = 0 these are very close to the centres of pressure of the corresponding monoplanes. The change in centre of pressure brought about by rolling to $\lambda = 45^\circ$ is small, being scarcely detectable in the case of $XB_{1a}W_8$, and amounting consistently to about 0.1 of a calibre for $XB_{1a}W_1$.

Variation of the initial lift curve slope and also of centre of pressure with Mach number is shown in Fig.6. The data at M = 4 are taken from the present Paper or from Ref.1, the data at other Mach numbers are taken from Refs.2 and 8.

The variation of axial force with incidence is shown in Fig.7. All configurations exhibit roughly the same behaviour with incidence. The differences in level are not simply proportional to exposed wing area. The discrepancies could be due in part to the drag of the roughness elements, which would be about the same for each wing, and partly to complications of boundary layer behaviour in the wing-body junctions.

Lift-drag ratios are presented in Fig.8 for the monoplanes. It is quite noticeable that even the smallest wings enhance L/D considerably. Figs.9(a) and 9(b) show corresponding values for the cruciform models. In both cases

---

*Normal force in this case is defined as in Fig.2; it is the force component acting in the incidence plane, normal to the axis of the model.

L/D is reduced, particularly at lower incidences, by the additional drag on the extra pair of wings. For both configurations $(L/D)_{max}$ is reduced by about 0.6. The effect of roll angle appears to be small.

Fig.10 shows that, for all configurations tested, C_D varies linearly with C_L^2 over the entire range of incidence studied. This is in contrast to the findings on these models at lower Mach numbers[2]. From the slopes of these lines, one may calculate the lift dependent drag factor, defined by

$$k = \frac{C_D - C_{D_o}}{C_L^2} \times \frac{4(\text{span})^2}{d^2}$$

where the span involved is the total span of the wing-body combination (2s in Fig.1). Values are as below

Monoplanes	k
$B_{1a}W_9$	1.2
$B_{1a}W_8$	1.4
$B_{1a}W_7$	2.1
$B_{1a}W_1$	2.9

Cruciform	$k_{\lambda = 45^o}$
$XB_{1a}W_8$	1.5
$XB_{1a}W_1$	3.0

3.2 Induced rolling moments

Plots of induced rolling moment against roll angle at various pitch attitudes are shown in Figs.11 and 12.

No data is available for $B_{1a}W_1$, but results for the other three monoplane configurations are presented in Figs.11(a)-(c). All these models were stable about the position $\lambda = 0$ at all pitch angles, but the actual moments are very non-linear with incidence, and it was not found possible to correlate them in any simple way.

Results for models $XB_{1a}W_1$ and $XB_{1a}W_8$ are presented in Figs.12(a) and (b) respectively. Both models are stable about $\lambda = 45^o$ at all incidences,

although again the actual values are too complicated to correlate. One coincidence, however, may be worth noting, and is suggested by the following argument.

The only pressures which can contribute to the rolling moment are those acting on the wing panels. The most significant contributions at high Mach number are likely to be those from the panels on the windward side. If the wings are small enough it may be assumed that these panels act independently of each other and of the leeward panels. If all these assumptions hold the rolling moments of cruciform and monoplane arrangements may be correlated as follows:-

$$\left(C_{\ell_X}\right)_{\lambda=\lambda_1} = \left(C_{\ell_M}\right)_{\lambda=\lambda_1} - \left(C_{\ell_M}\right)_{\lambda=\frac{\pi}{2}-\lambda_1} .$$

The results of Fig.11(b) for model $B_{1a}W_8$ have been used to predict results for model $XB_{1a}W_8$ by means of this formula, and the resulting estimates shown in Fig.12(b). Agreement is fair, considering the drastic simplifications involved, and the sense of stability is predicted correctly.

4 CONCLUSIONS

(1) As aspect ratio decreases, the variation of normal force with incidence becomes increasingly non-linear, and centre of pressure travel is increased.

(2) Calculated values of normal force and centre of pressure agree with experiment to within 8% and 0.2 calibres respectively, except for the body alone.

(3) For the cruciform configurations considered, longitudinal characteristics depend relatively little on roll angle.

(4) Lift-drag ratio is much improved by the addition of even the smallest wings. The cruciform models reached maximum lift-drag ratios about 0.6 less than those of the corresponding monoplanes.

(5) The monoplane models are stable in roll about $\lambda = 0$, the cruciform models about $\lambda = 45^{\circ}$.

SYMBOLS

C_D	drag coefficient = $4 \times (\text{drag})/q_\infty \pi d^2$
C_ℓ	rolling moment coefficient (body axes) = $4 \times (\text{rolling moment})/q_\infty \pi d^3$
$-C_x$	axial force coefficient = $4 \times (\text{axial force})/q_\infty \pi d^2$
$-C_z$	normal force coefficient (body axes) = $4 \times (\text{normal force})/q_\infty \pi d^2$
$-C'_z$	normal force coefficient (resolved body axes)
$\frac{dC_z}{d\alpha}$	normal force coefficient slope vs incidence (per radian)
d	body diameter
L/D	lift-drag ratio
M	free stream Mach number
q_∞	free stream dynamic pressure
$x_{c.p.}$	distance of centre of pressure from wing trailing edge
α	angle of incidence
σ	angle between body axis and wind vector
λ	angle between plane normal to wing surface containing body axis and plane containing body axis and wind vector
ϕ	wing leading edge sweepback angle

REFERENCES

No.	Author	Title, etc.
1	D.R. Andrews	Guided Weapons Aerodynamic Study; force and moment measurements on three delta wings of aspect ratio 0.83, 1.03, and 1.24 in combination with bodies of fineness ratio 13 at a Mach number of 4.0. ARC CP 888, April 1962
2	J.B. Ogle	Guided Weapons Aerodynamic Study; force tests on four slender delta wing bodies at Mach numbers from 0.6 to 2.8, and a method of predicting the longitudinal characteristics. RAE Technical Report 66307, ARC 28706, October 1966
3	J.R. Collingbourne	An empirical prediction method for non-linear normal force on thin wings at supersonic speeds. ARC CP 662, January 1962
4	W.C. Pitts J.N. Nielsen G.G. Kaatari	Lift and centre of pressure of wing-body-tail combinations at subsonic, transonic and supersonic speeds. NACA Report 1307, 1957
5	T.M.F. Moore	A review of empirical prediction methods for the longitudinal aerodynamic characteristics at zero roll of slender wing-body combinations at supersonic speeds. B.A.C.(O) Ltd. Final Report Research Contract KVB/363/CB/64a (to be published)
6	H.J. Allen	Estimation of the forces and moments acting on inclined bodies of revolution of high fineness ratio. Unpublished NACA Report
7	-	Royal Aeronautical Society Data Sheets. Aerodynamics Vol.2
8	W.K. Osborne	Guided Weapons Aerodynamic Study; tests on a body alone, and in combination with delta-wings of aspect ratio 0.83, 1.03 and 1.24 at Mach numbers up to 2.8. RAE Technical Report 65109, ARC 27228, June 1965

WING	SPAN (2S)
1	5d
7	3·5d
8	2·5d
9	2·11d

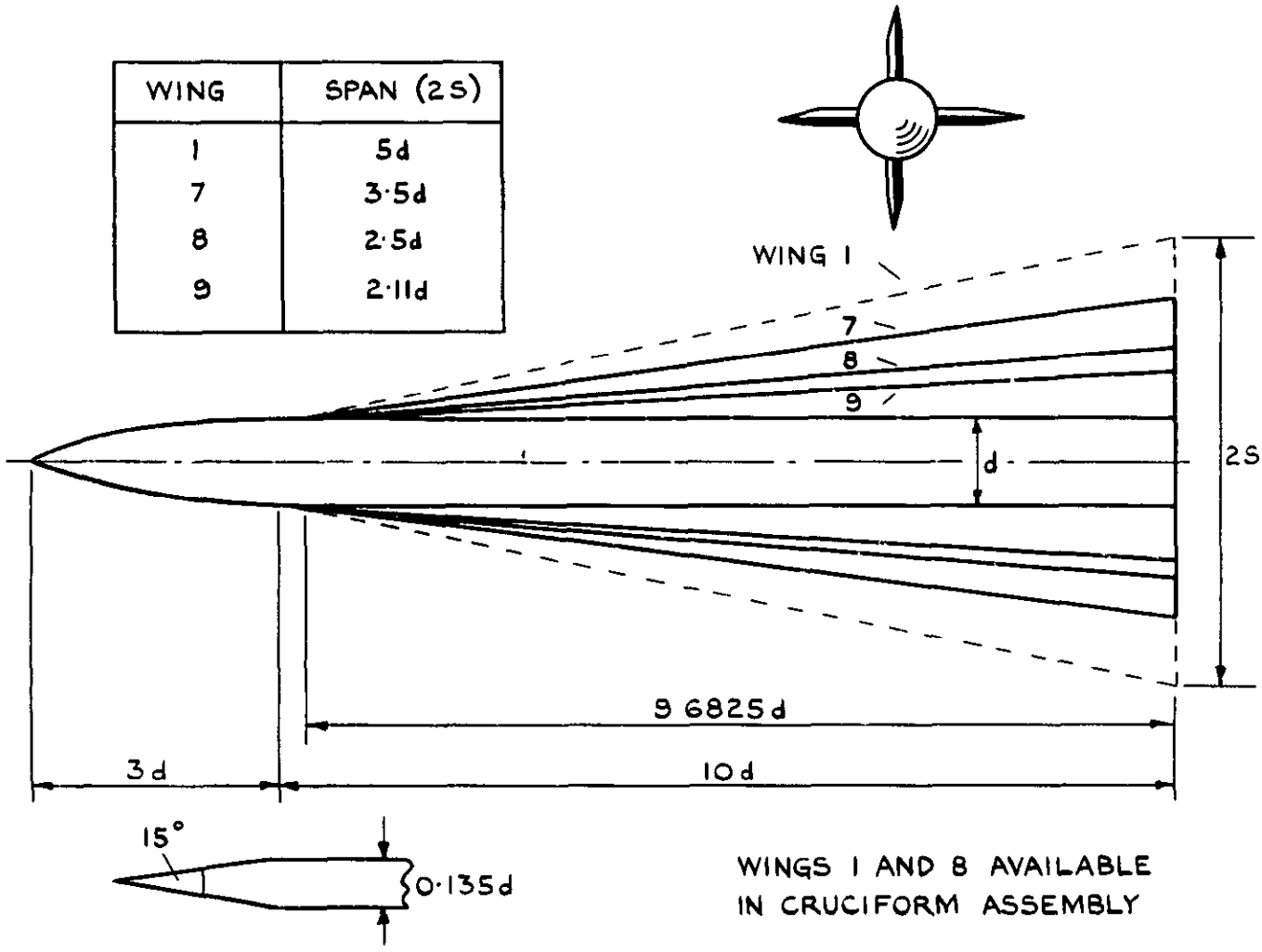

FIG. 1 MODEL GEOMETRY

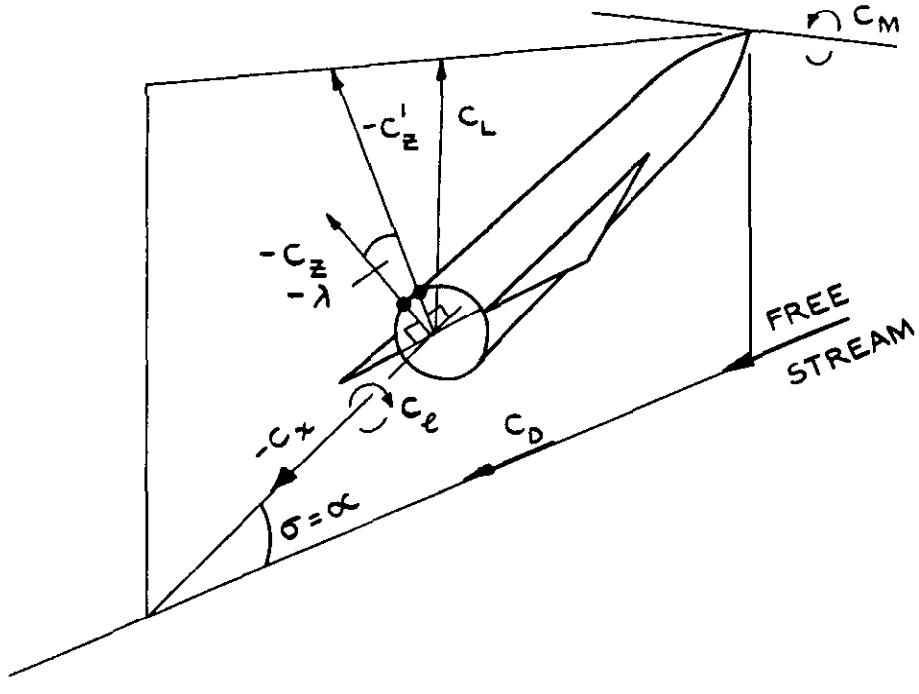

FIG. 2 AXIS SYSTEMS

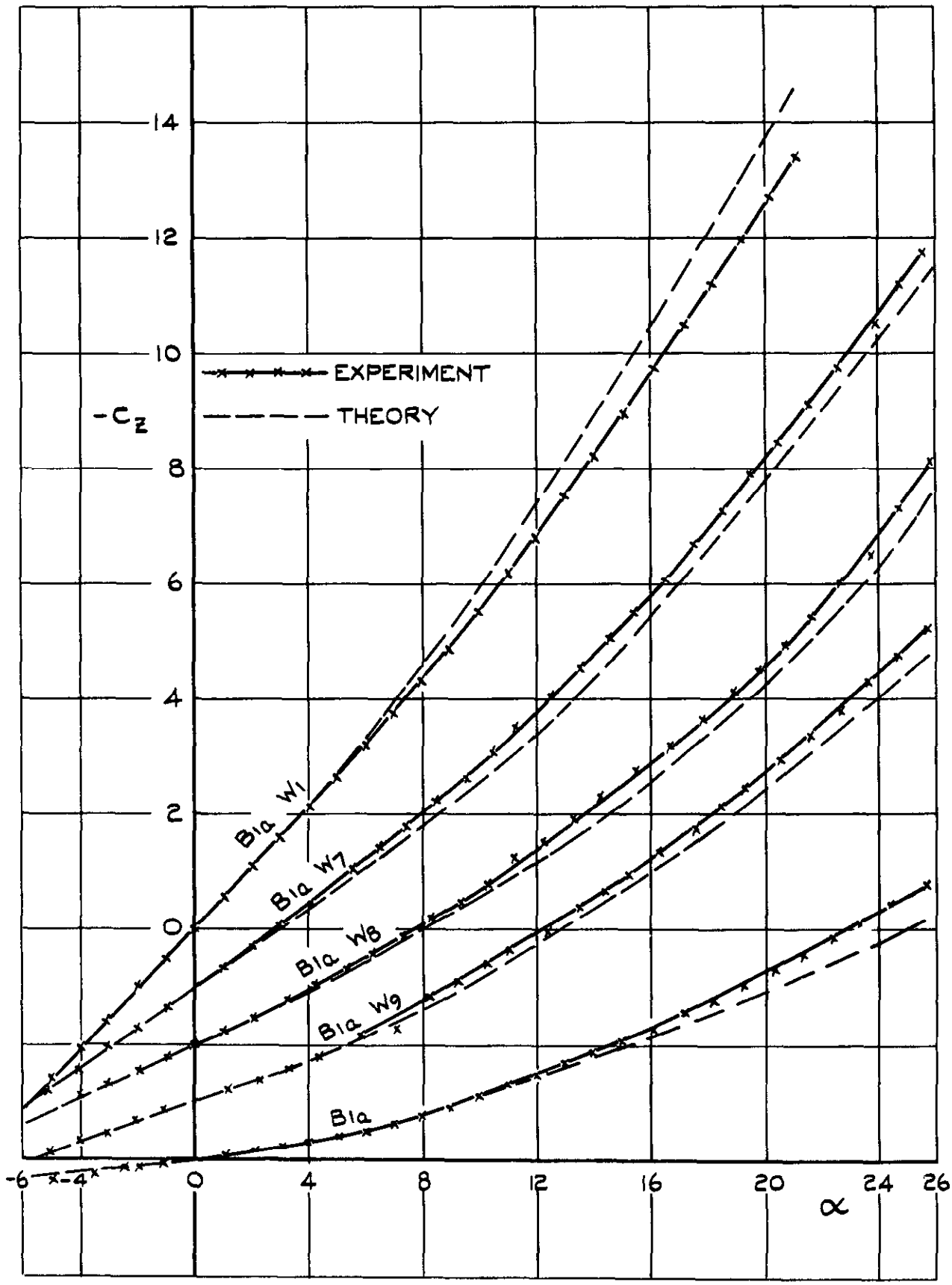

FIG. 3 NORMAL FORCE vs INCIDENCE
FOR MONOPLANE CONFIGURATIONS

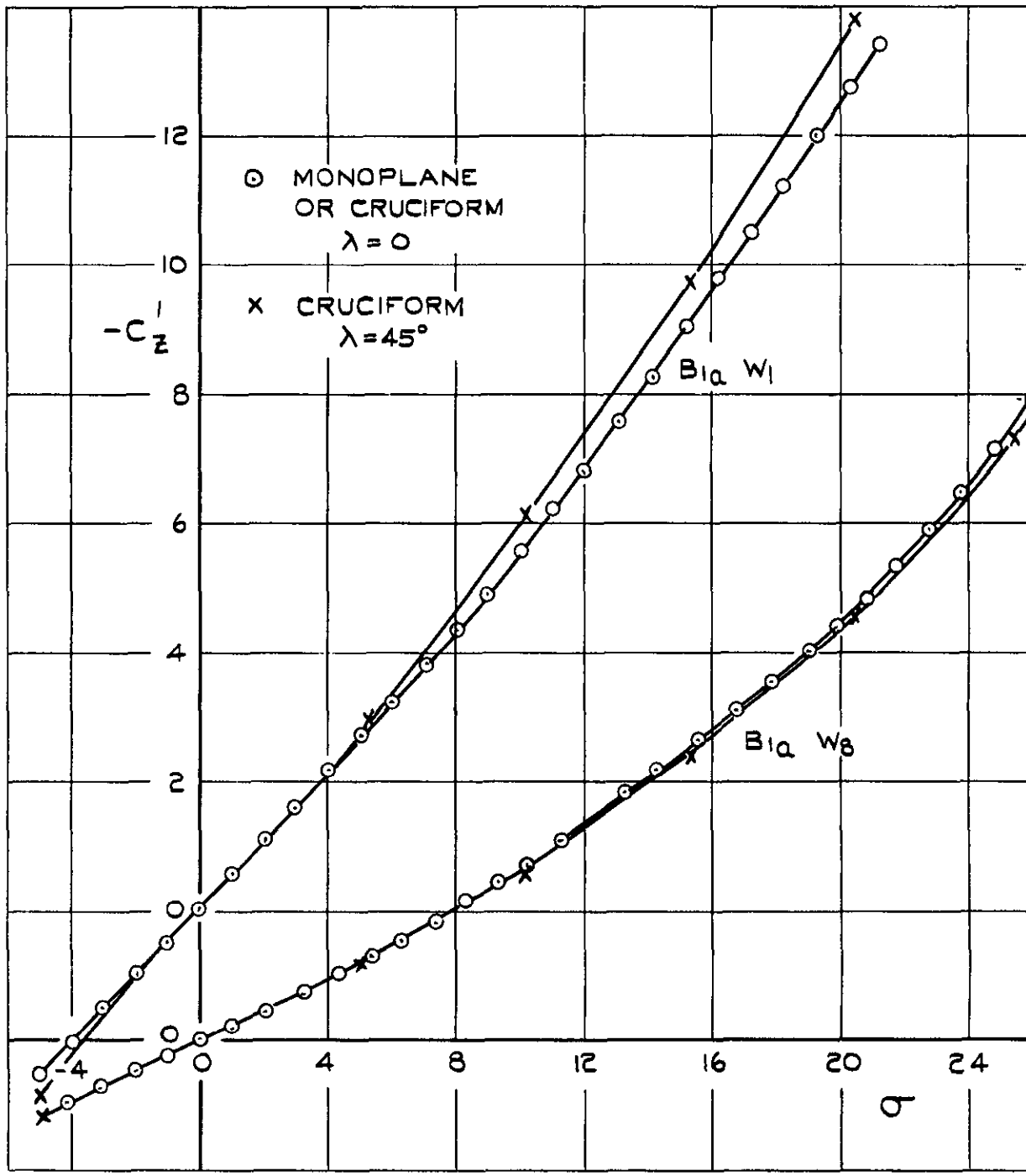

FIG.4 NORMAL FORCE vs RESOLVED INCIDENCE
(MONOPLANE AND CRUCIFORM)

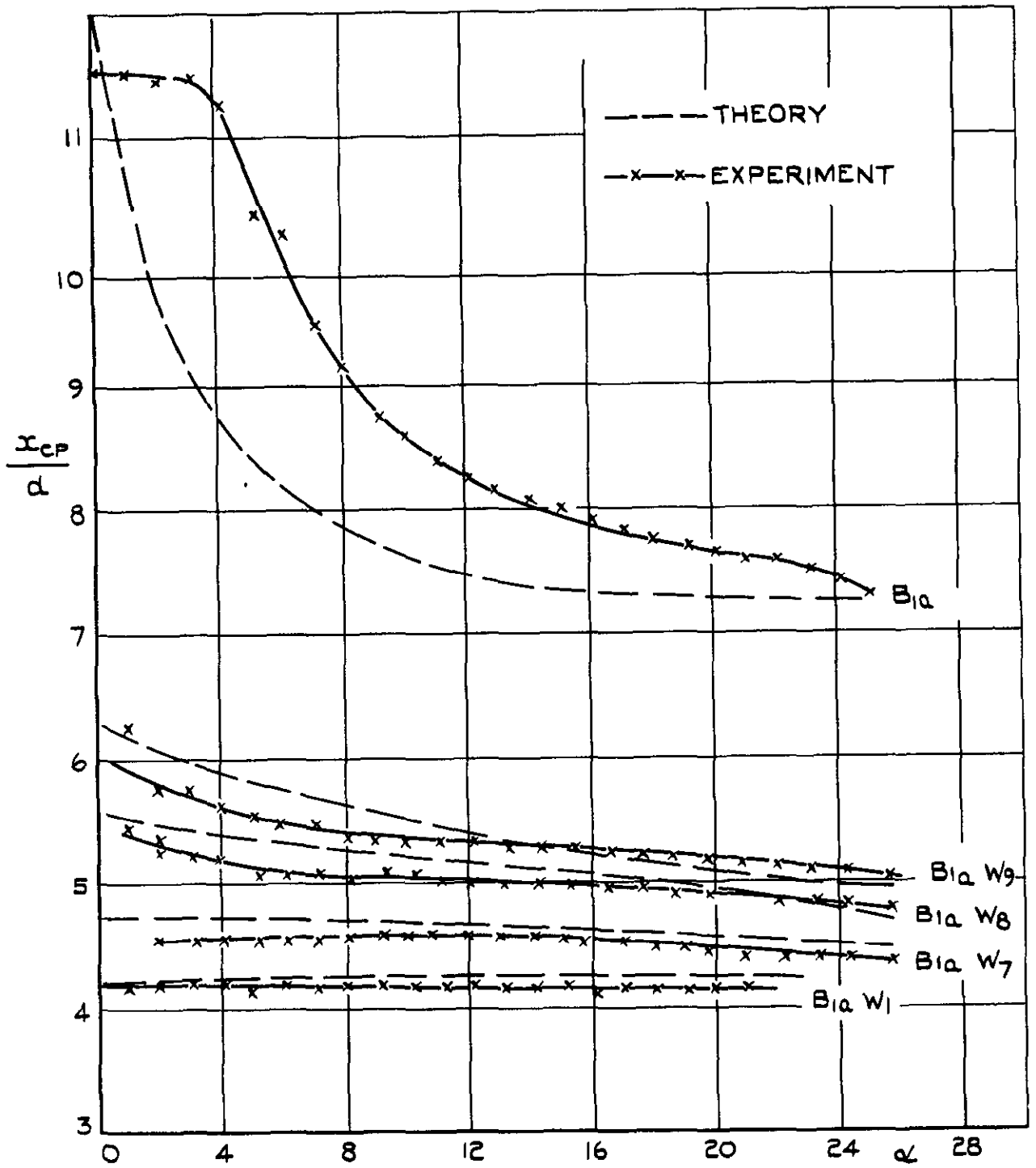

FIG.5 (a) MONOPLANES

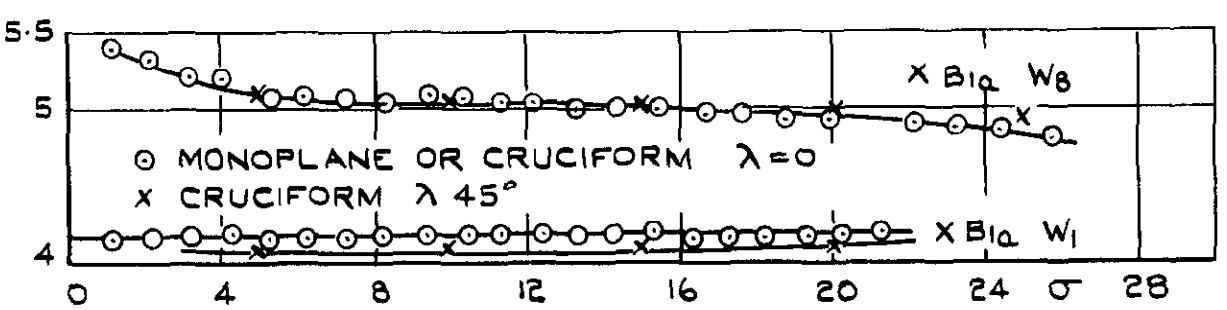

FIG.5 (b) CRUCIFORM CONFIGURATIONS

FIG.5 CENTRE OF PRESSURE vs INCIDENCE
(x MEASURED FORWARD FROM TRAILING EDGE)

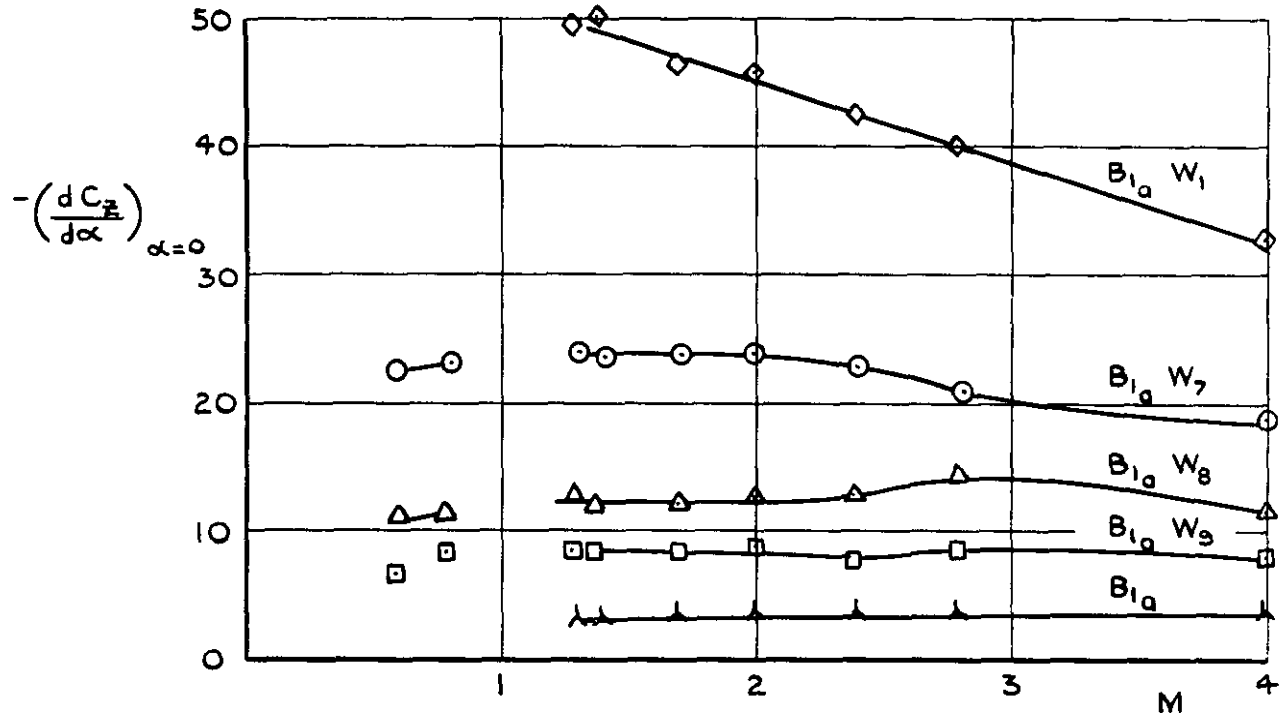

FIG 6(a) INITIAL LIFT CURVE SLOPE

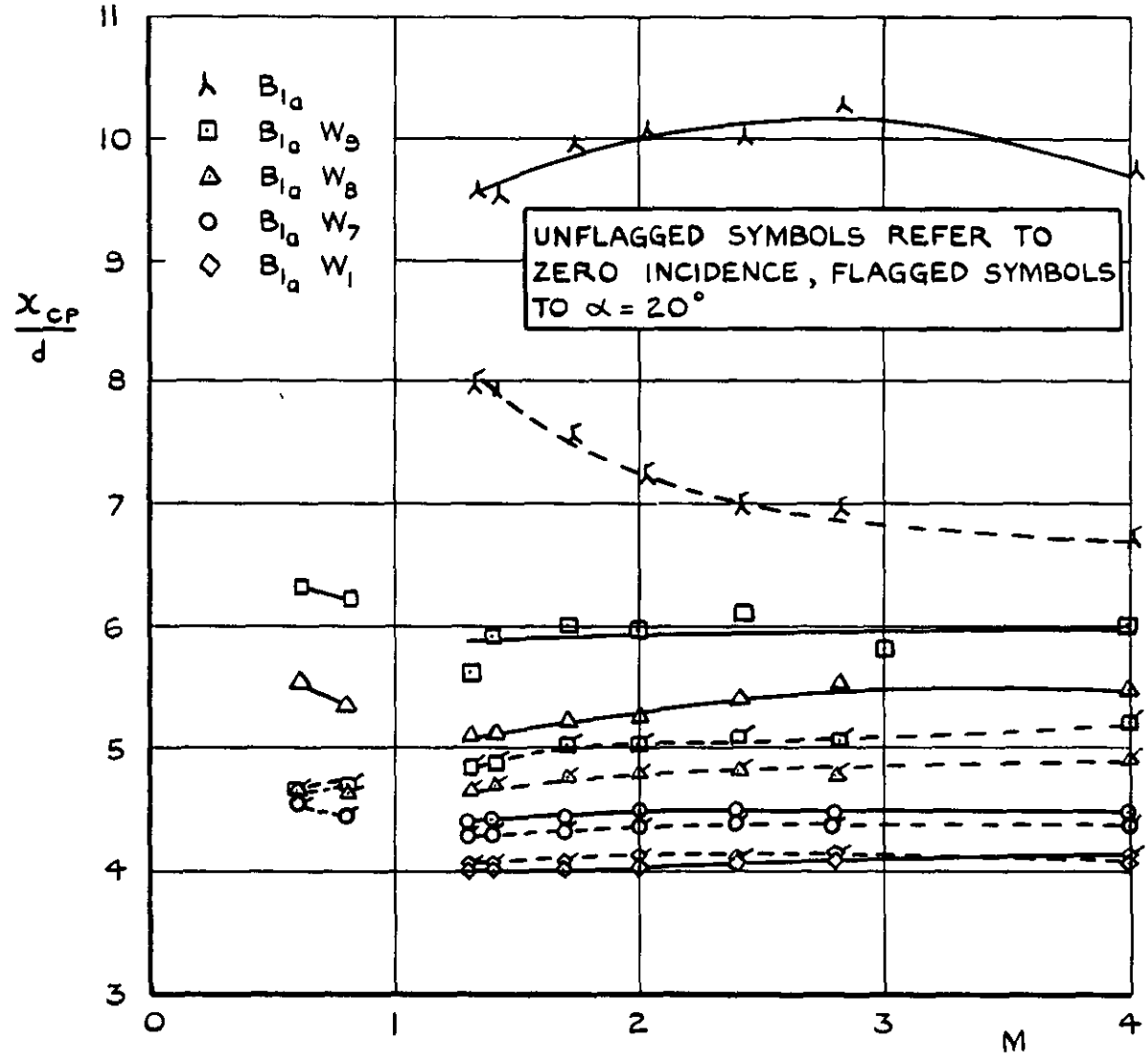

FIG.6(b) CENTRE OF PRESSURE

FIG. 6 VARIATION OF LONGITUDINAL CHARACTERISTICS WITH MACH NUMBER

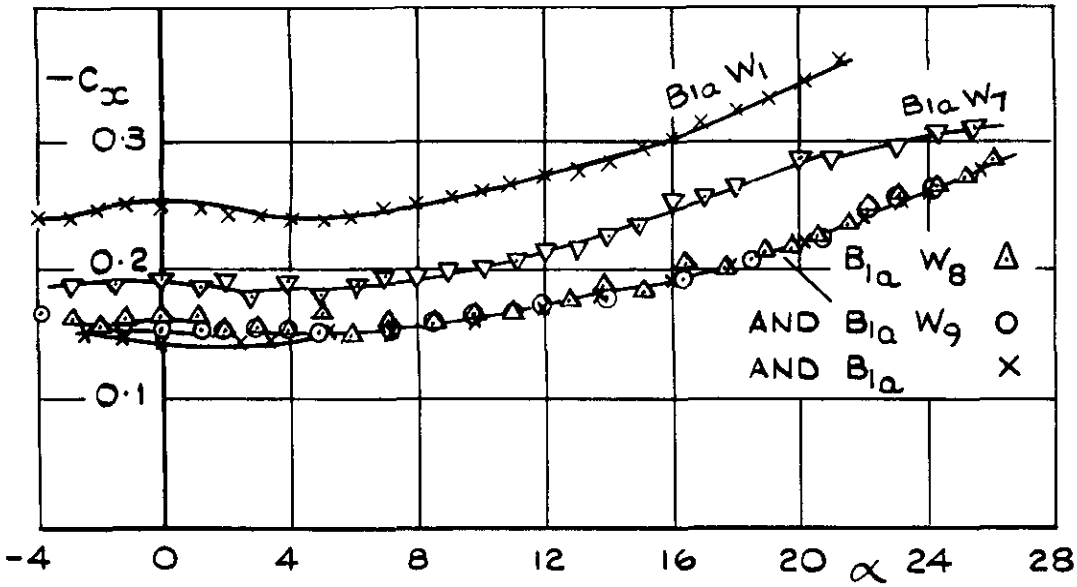

FIG.7 (a) MONOPLANE CONFIGURATIONS

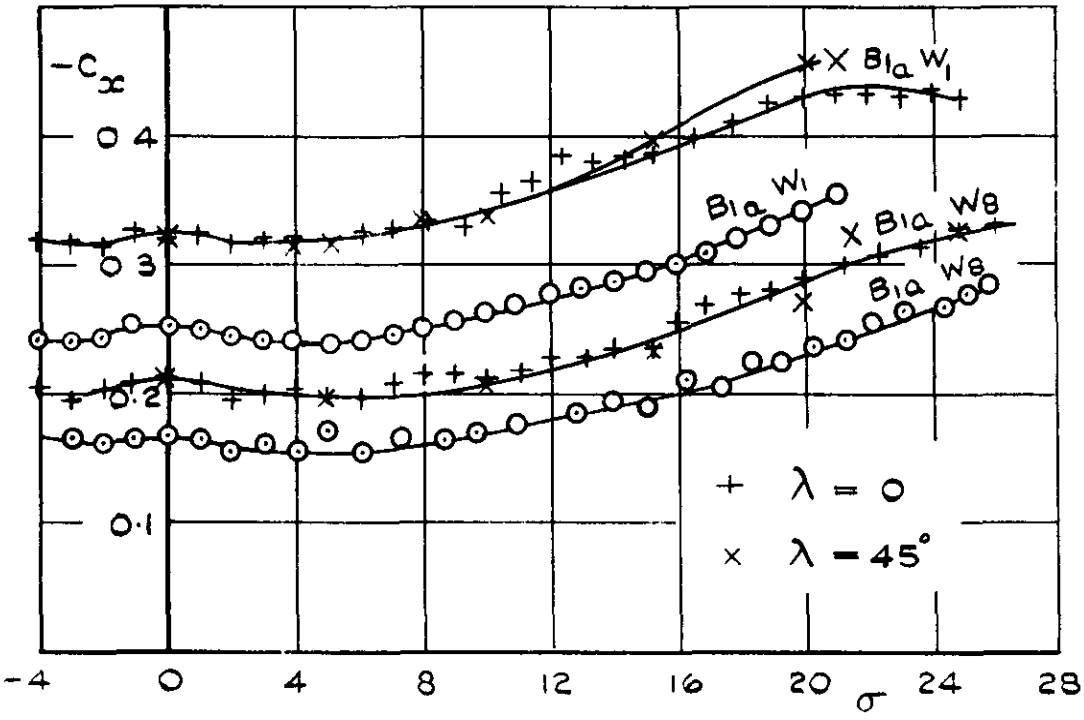

FIG.7 (b) CRUCIFORM CONFIGURATIONS

FIG.7 AXIAL FORCE VS INCIDENCE

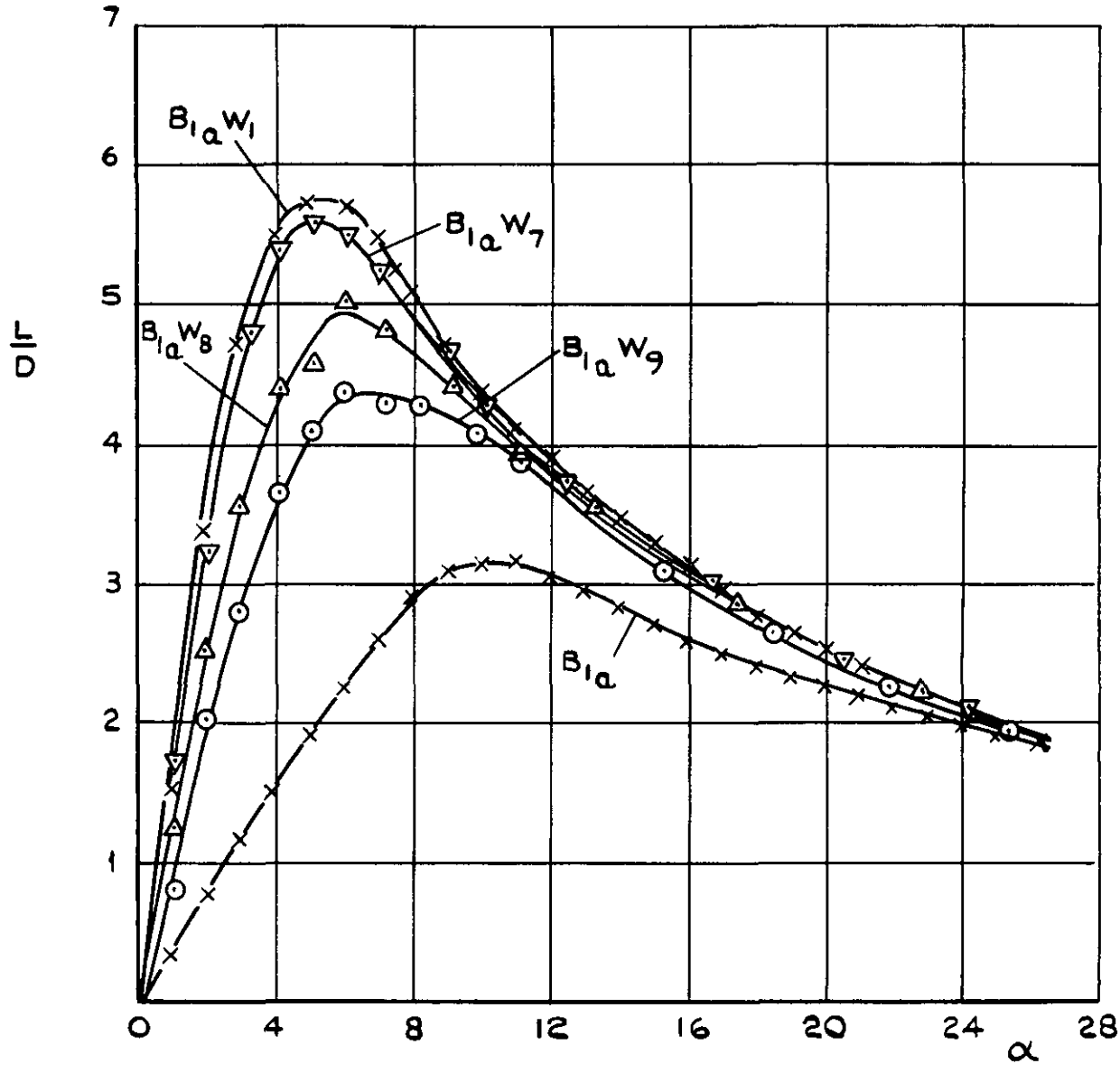

FIG. 8 LIFT-DRAG RATIO VS INCIDENCE FOR MONOPLANE CONFIGURATIONS

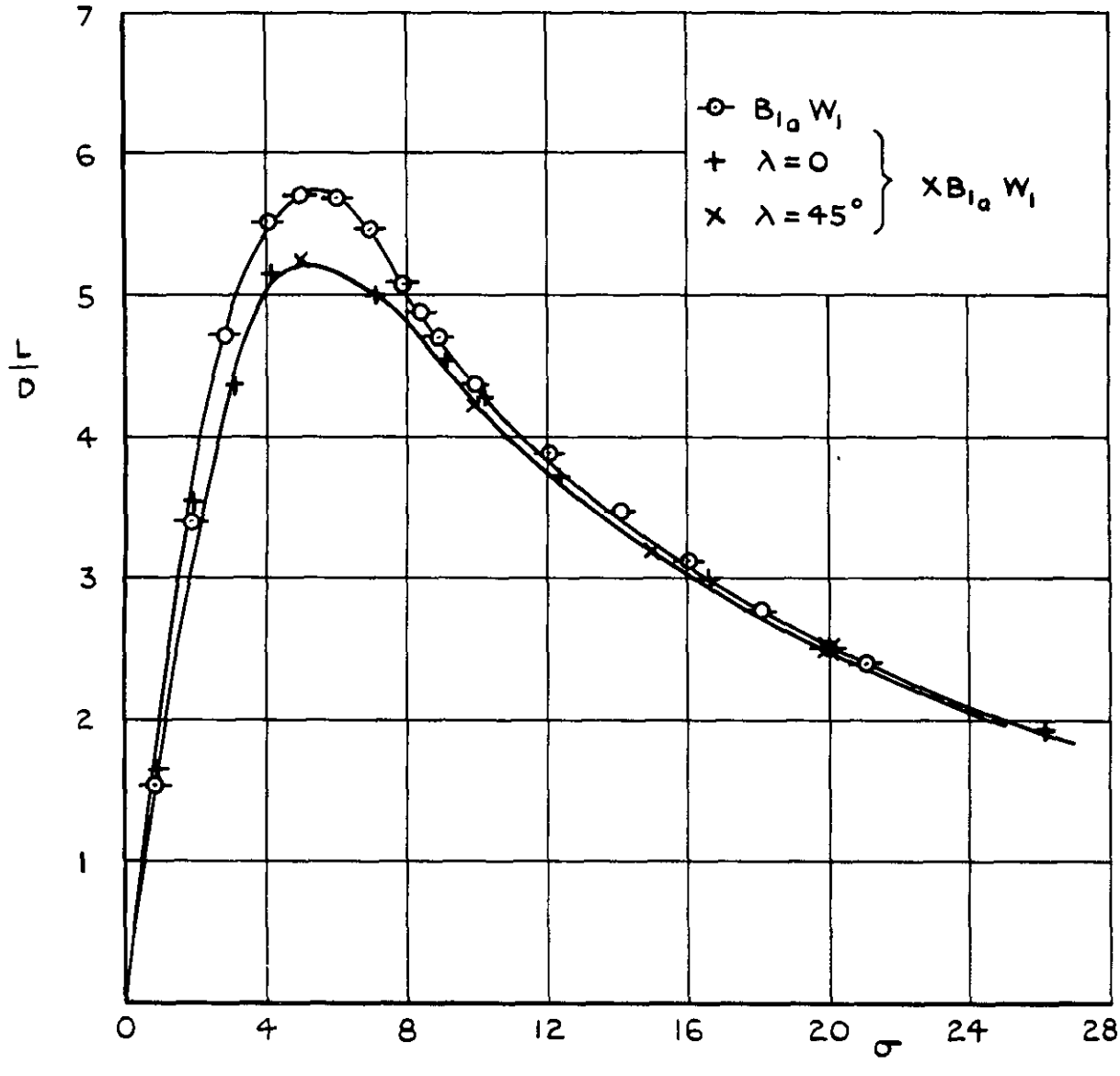

FIG.9 (a) B_{1a} W_1 AND XB_{1a} W_1

FIG.9 LIFT- DRAG RATIO vs INCIDENCE

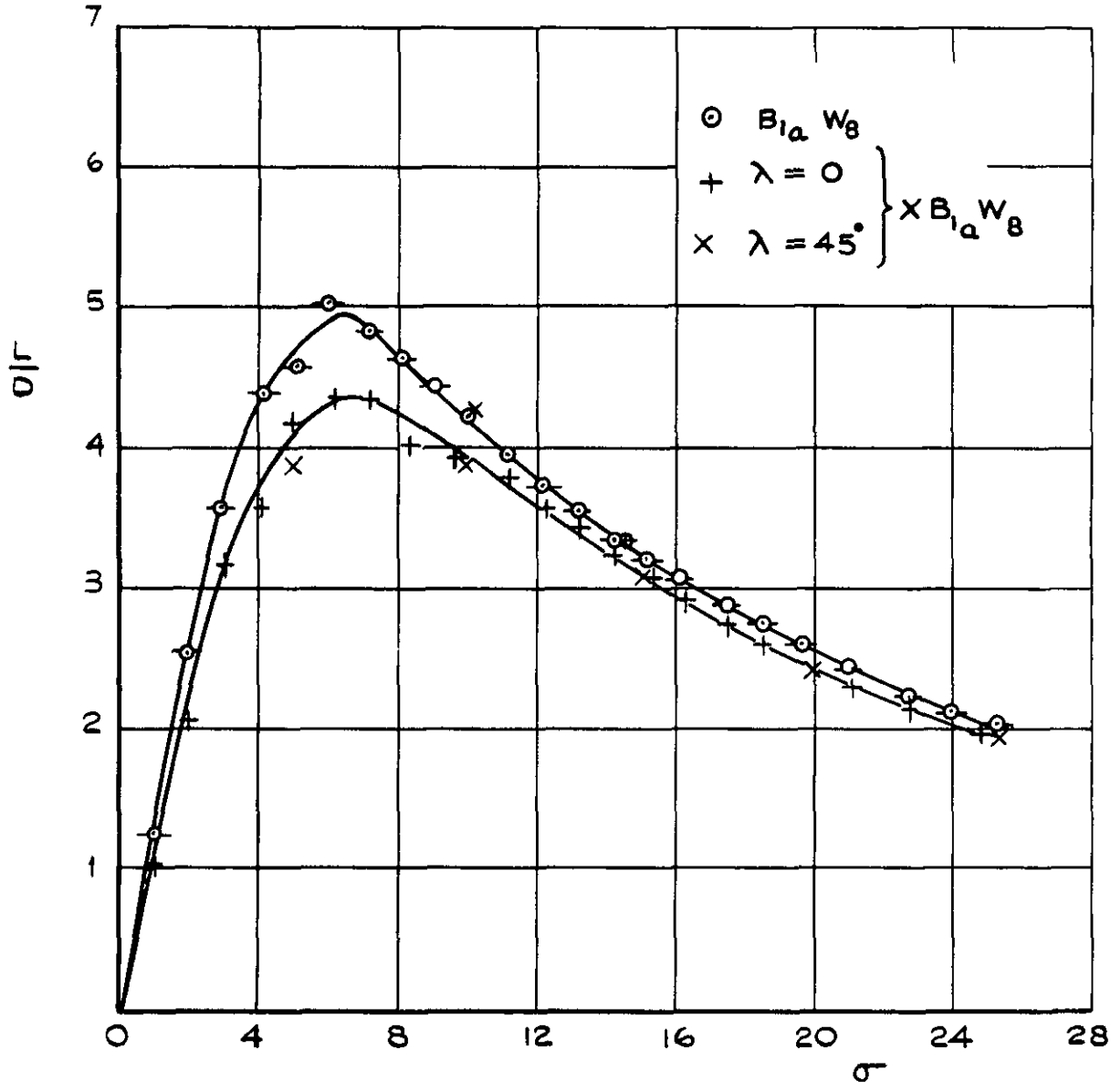

FIG.9 (b) B_{1a} W_8 AND XB_{1a} W_8

FIG.9 LIFT-DRAG RATIO VS INCIDENCE

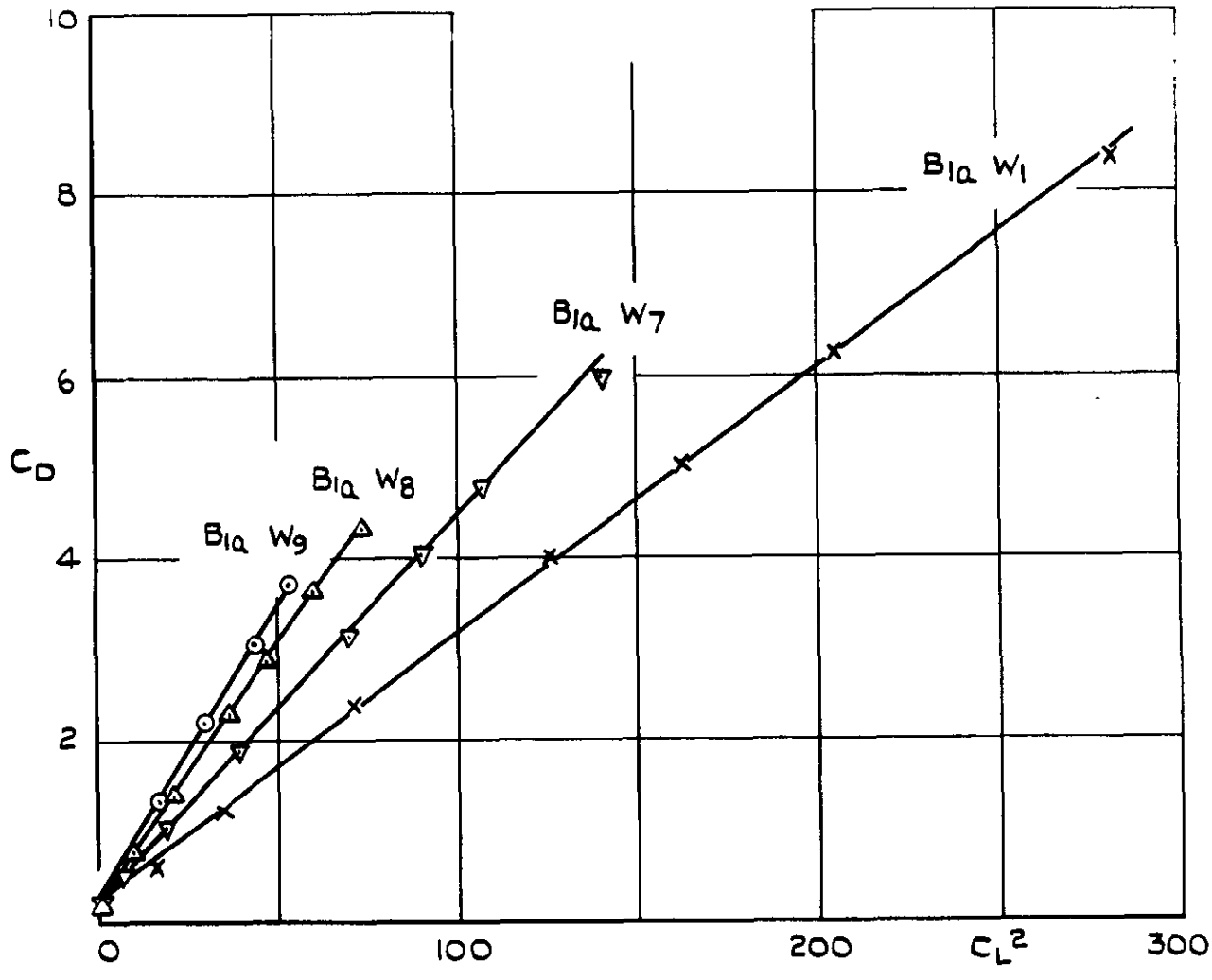

FIG. 10 (a) MONOPLANES

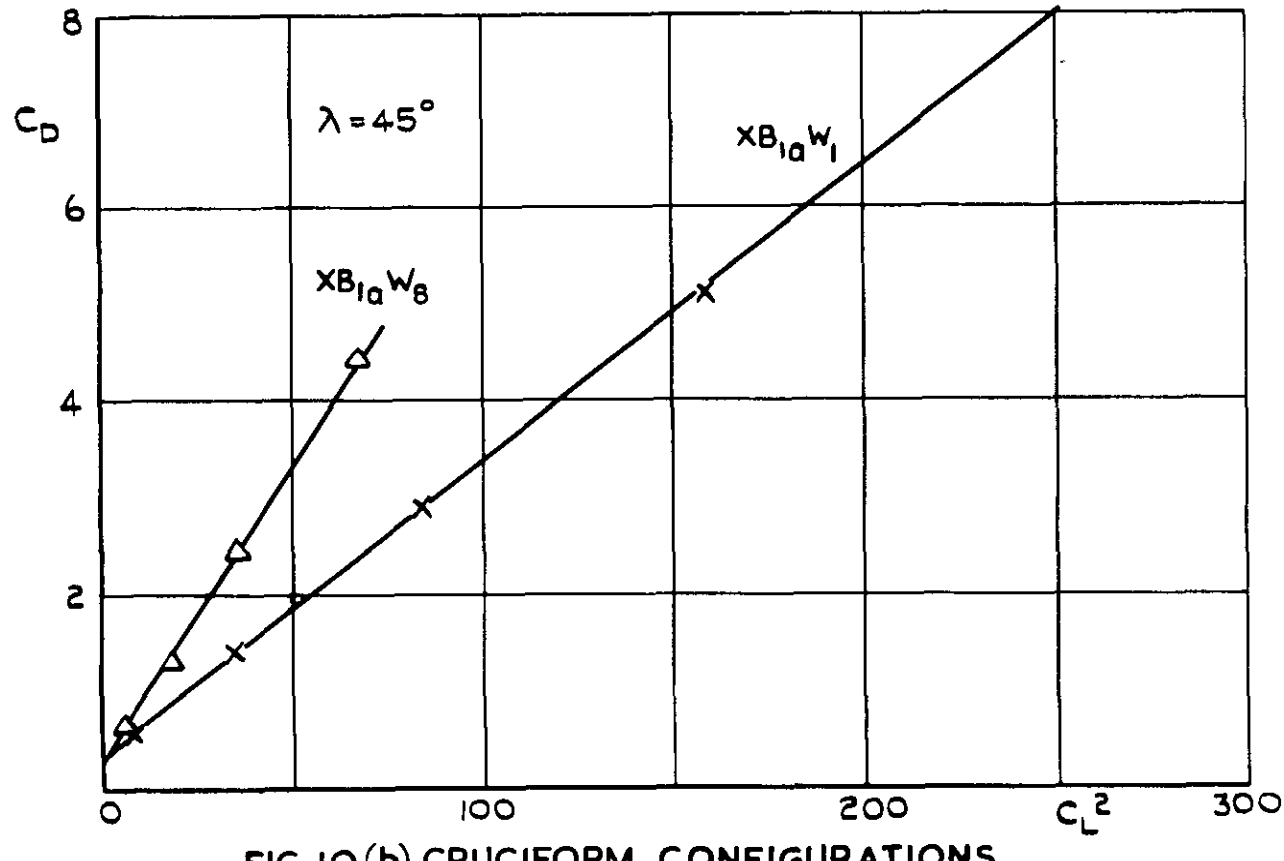

FIG. 10 (b) CRUCIFORM CONFIGURATIONS

FIG. 10 C_D vs C_L^2

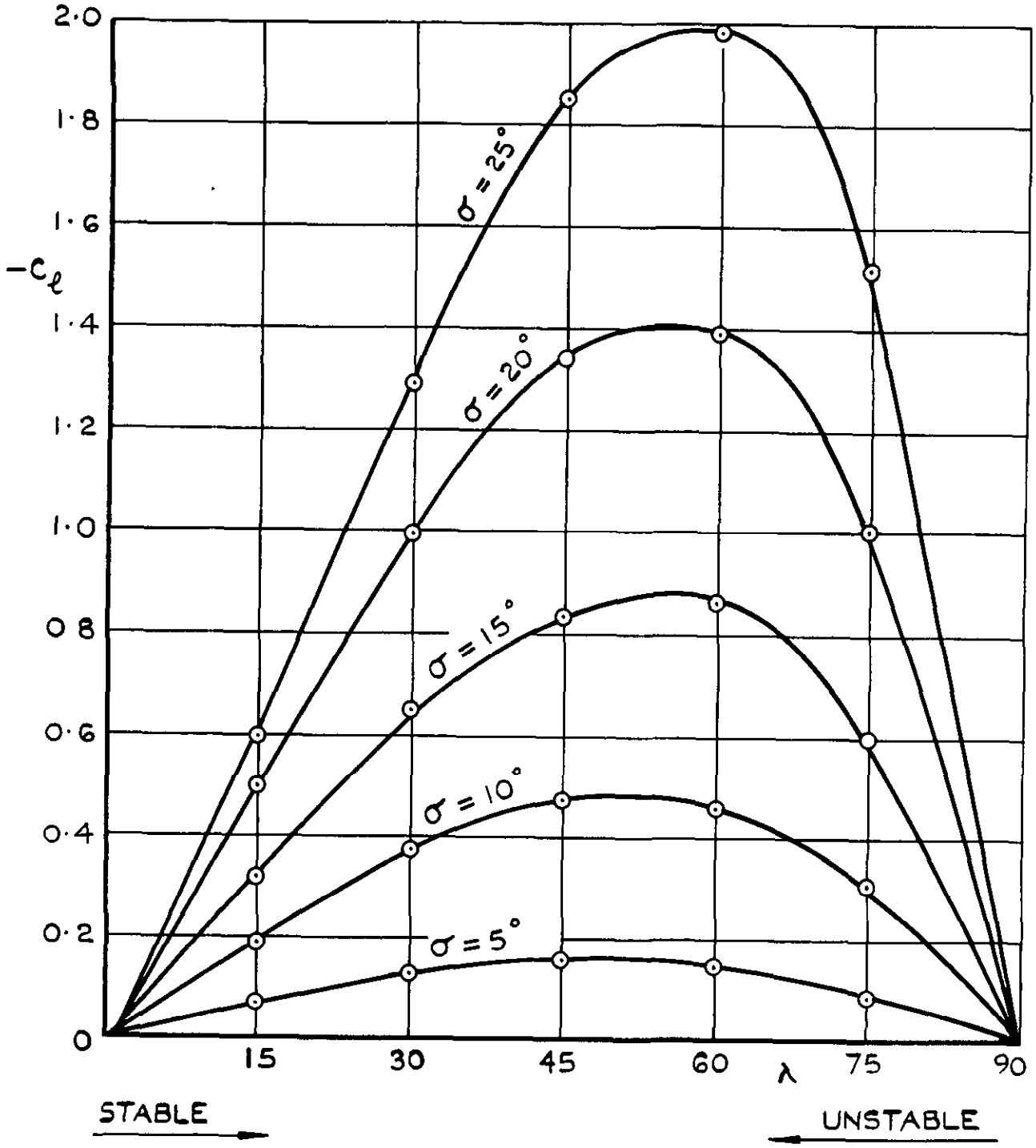

FIG. 11 (a) B_{1a} W_7

FIG 11 INDUCED ROLLING MOMENT VS ROLL ANGLE (MONOPLANES)

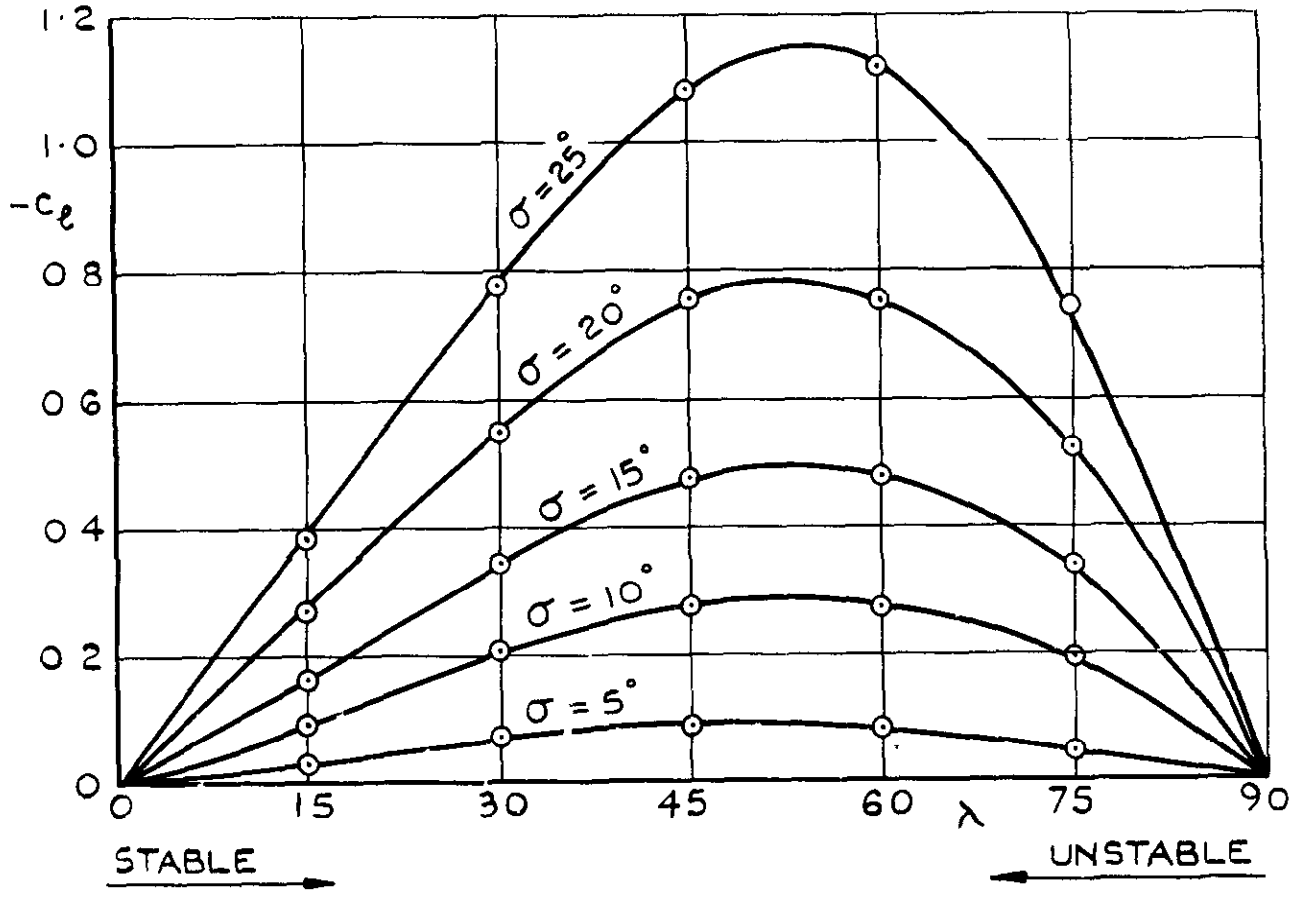

FIG.11 (b) B_{1a} W_8

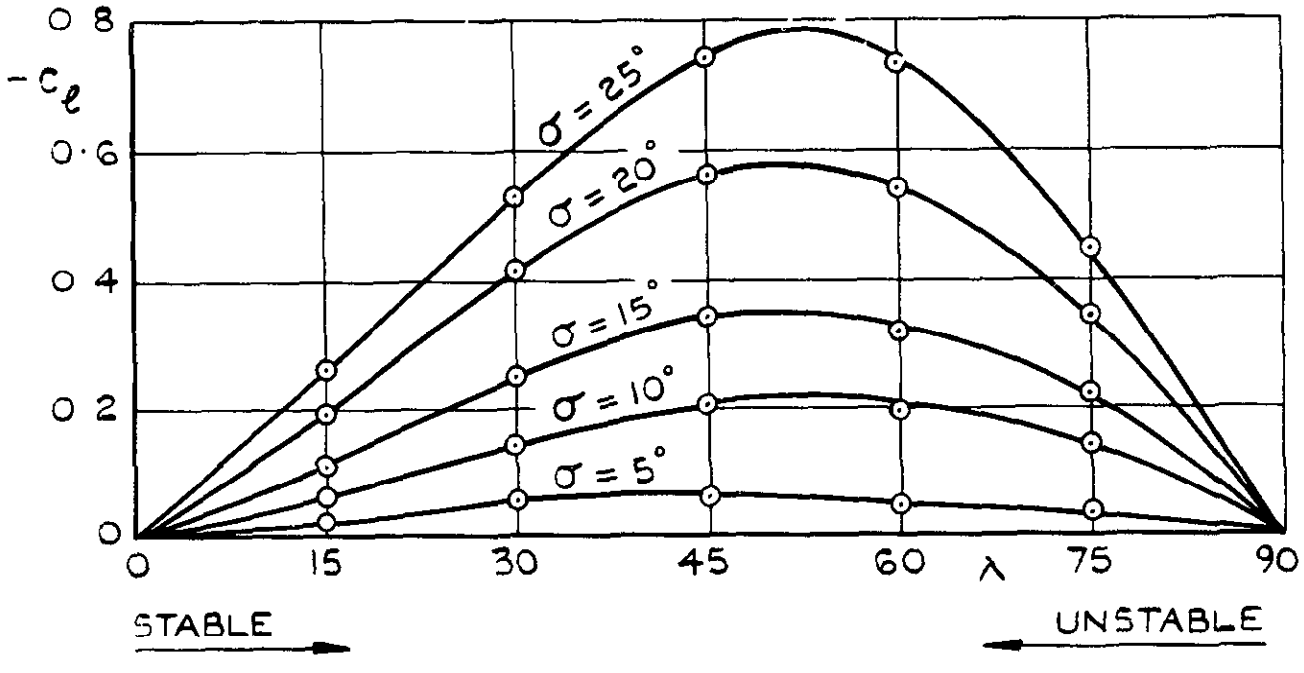

FIG 11 (c) B_{1a} W_9

FIG 11 (CONT'D) INDUCED ROLLING MOMENT VS ROLL ANGLE (MONOPLANES)

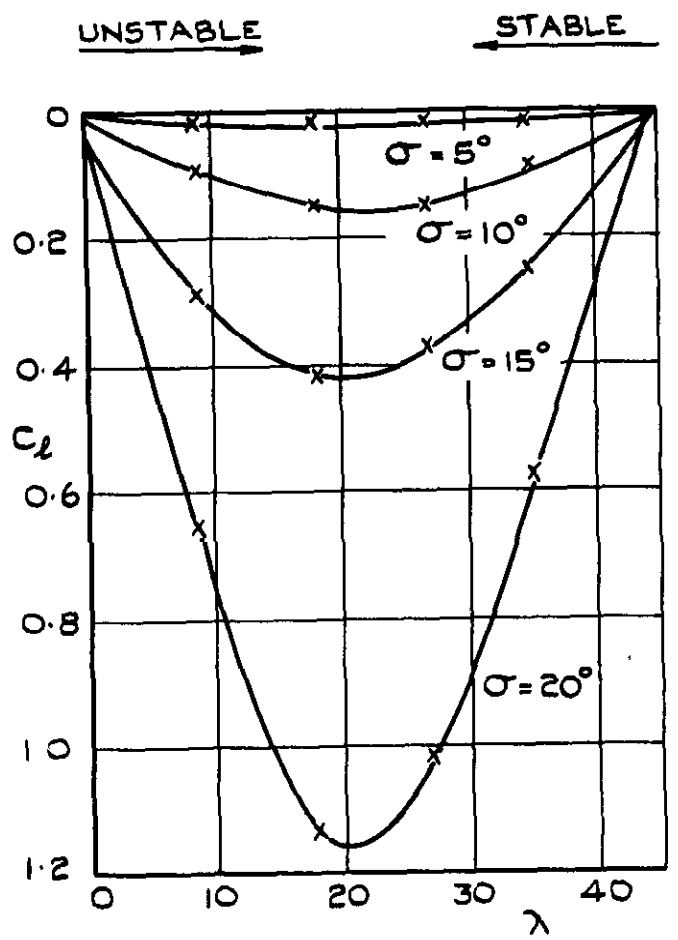

FIG. 12 (a) $XB_{1a}W_1$

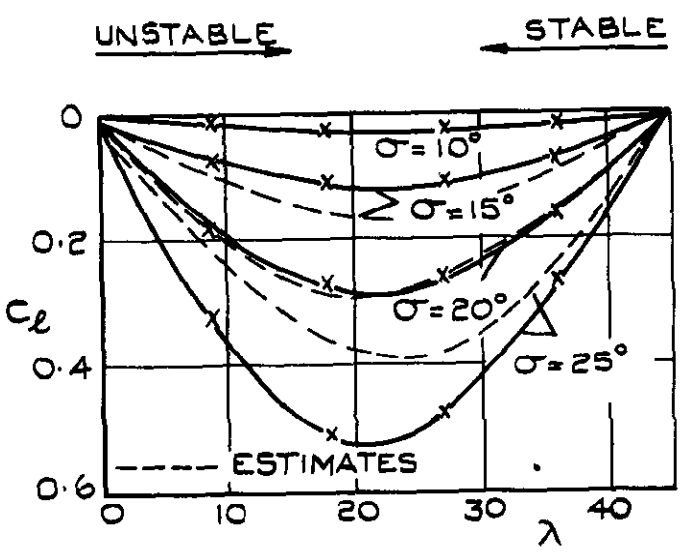

FIG. 12 (b) $XB_{1a}W_8$

FIG. 12 INDUCED ROLLING MOMENT vs ROLL ANGLE (CRUCIFORM)

Printed in England for Her Majesty's Stationery Office by the Royal Aircraft Establishment, Farnborough. Dd.128528. K.4.

A.R.C. C.P. No.972
October 1966

Roe, P.L.

FORCE AND MOMENT MEASUREMENTS ON SOME MONOPLANE AND CRUCIFORM SLENDER WING-BODY COMBINATIONS AT M = 4.0

533.665 : 533.695.12 : 533.693.3 : 533.6.013.13/15 : 533.693.9 : 533.652.1 : 533.6.011.5

Force and moment measurements are presented for a family of slender delta monoplane wings (aspect ratios 0.826, 0.517, 0.309, 0.229) in combination with a common ogive-cylinder body. Two of these (aspect ratios 0.826 and 0.309) are also studied in cruciform layout. Results are given for variations in incidence at zero roll, and variations in roll at constant pitch. Longitudinal characteristics are compared with an empirical prediction method, and with test results at lower Mach numbers.

A.R.C. C.P. No.972
October 1966

Roe, P.L.

FORCE AND MOMENT MEASUREMENTS ON SOME MONOPLANE AND CRUCIFORM SLENDER WING-BODY COMBINATIONS AT M = 4.0

533.665 : 533.695.12 : 533.693.3 : 533.6.013.13/15 : 533.693.9 : 533.652.1 : 533.6.011.5

Force and moment measurements are presented for a family of slender delta monoplane wings (aspect ratios 0.826, 0.517, 0.309, 0.229) in combination with a common ogive-cylinder body. Two of these (aspect ratios 0.826 and 0.309) are also studied in cruciform layout. Results are given for variations in incidence at zero roll, and variations in roll at constant pitch. Longitudinal characteristics are compared with an empirical prediction method, and with test results at lower Mach numbers.

A.R.C. C.P. No.972
October 1966

Roe, P.L.

FORCE AND MOMENT MEASUREMENTS ON SOME MONOPLANE AND CRUCIFORM SLENDER WING-BODY COMBINATIONS AT M = 4.0

533.665 : 533.695.12 : 533.693.3 : 533.6.013.13/15 : 533.693.9 : 533.652.1 : 533.6.011.5

Force and moment measurements are presented for a family of slender delta monoplane wings (aspect ratios 0.826, 0.517, 0.309, 0.229) in combination with a common ogive-cylinder body. Two of these (aspect ratios 0.826 and 0.309) are also studied in cruciform layout. Results are given for variations in incidence at zero roll, and variations in roll at constant pitch. Longitudinal characteristics are compared with an empirical prediction method, and with test results at lower Mach numbers.

Published by
HER MAJESTY'S STATIONERY OFFICE

To be purchased from
49 High Holborn, London W.C 1
423 Oxford Street, London W.1
13A Castle Street, Edinburgh 2
109 St. Mary Street, Cardiff
Brazennose Street, Manchester 2
50 Fairfax Street, Bristol 1
258-259 Broad Street, Birmingham 1
7-11 Linenhall Street, Belfast 2
or through any bookseller

C.P. No. 972

S.O. CODE No. 23-9017-72